ACCOUNTS of chemical research

Article

pubs.acs.org/accounts

Networks of Semiconducting SWNTs: Contribution of Midgap Electronic States to the Electrical Transport

Mikhail E. Itkis,*[,†,‡] Aron Pekker,[†,‡] Xiaojuan Tian,[†,§] Elena Bekyarova,[†,‡] and Robert C. Haddon*[,†,‡,§]

[†]Department of Chemistry, University of California, Riverside, California 92521, United States

[‡]Center for Nanoscale Science and Engineering, University of California, Riverside, California 92521, United States

[§]Department of Chemical Engineering, University of California, Riverside, California 92521, United States

Supporting Information

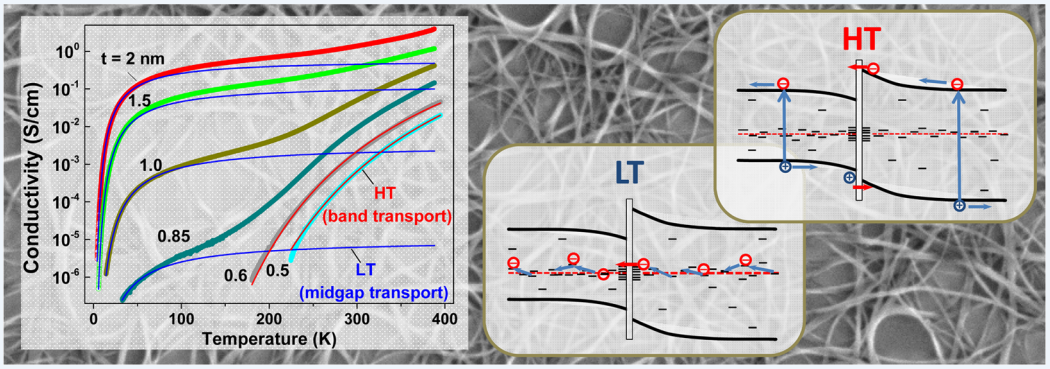

CONSPECTUS: Single-walled carbon nanotube (SWNT) thin films provide a unique platform for the development of electronic and photonic devices because they combine the advantages of the outstanding physical properties of individual SWNTs with the capabilities of large area thin film manufacturing and patterning technologies. Flexible SWNT thin film based field-effect transistors, sensors, detectors, photovoltaic cells, and light emitting diodes have been already demonstrated, and SWNT thin film transparent, conductive coatings for large area displays and smart windows are under development. While chirally pure SWNTs are not yet commercially available, the marketing of semiconducting (SC) and metallic (MT) SWNTs has facilitated progress toward applications by making available materials of consistent electronic structure. Nevertheless the electrical transport properties of networks of separated SWNTs are inferior to those of individual SWNTs. In particular, for semiconducting SWNTs, which are the subject of this Account, the electrical transport drastically differs from the behavior of traditional semiconductors: for example, the bandgap of germanium (E = 0.66 eV) roughly matches that of individual SC-SWNTs of diameter 1.5 nm, but in the range 300−100 K, the intrinsic carrier concentration in Ge decreases by more than 10 orders of magnitude while the conductivity of a typical SC-SWNT network decreases by less than a factor of 4. Clearly this weak modulation of the conductivity hinders the application of SC-SWNT films as field effect transistors and photodetectors, and it is the purpose of this Account to analyze the mechanism of the electrical transport leading to the unusually weak temperature dependence of the electrical conductivity of such networks. Extrinsic factors such as the contribution of residual amounts of MT-SWNTs arising from incomplete separation and doping of SWNTs are evaluated. However, the observed temperature dependence of the conductivity indicates the presence of midgap electronic states in the semiconducting SWNTs, which provide a source of low-energy excitations, which can contribute to hopping conductance along the nanotubes following fluctuation induced tunneling across the internanotube junctions, which together dominate the low temperature transport and limit the resistivity of the films. At high temperatures, the intrinsic carriers thermally activated across the bandgap as in a traditional semiconductor became available for band transport. The midgap states pin the Fermi level to the middle of the bandgap, and their origin is ascribed to defects in the SWNT walls. The presence of such midgap states has been reported in connection with scanning tunneling spectroscopy experiments, Coulomb blockade observations in low temperature electrical measurements, selective electrochemical deposition imaging, tip-enhanced Raman spectroscopy, high resolution photocurrent spectroscopy, and the modeling of the electronic density of states associated with various defects.

Midgap states are present in conventional semiconductors, but what is unusual in the present context is the extent of their contribution to the electrical transport in networks of semiconducting SWNTs. In this Account, we sharpen the focus on the midgap states in SC-SWNTs, their effect on the electronic properties of SC-SWNT networks, and the importance of these effects on efforts to develop electronic and photonic applications of SC-SWNTs.

Received: February 27, 2015
Published: August 5, 2015

DOI: 10.1021/acs.accounts.5b00107
Acc. Chem. Res. 2015, 48, 2270−2279

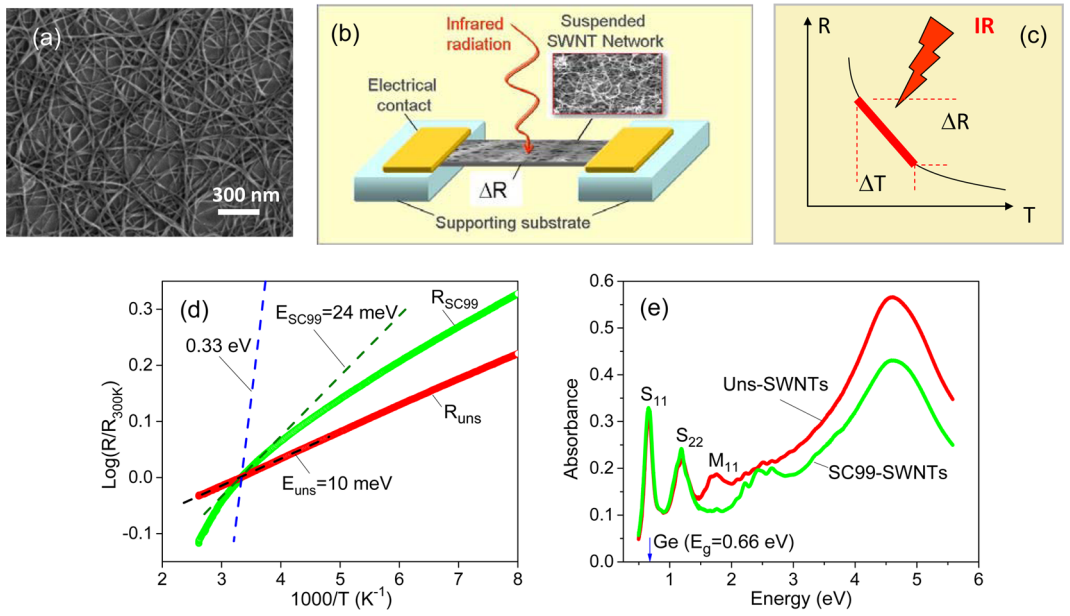

Figure 1. (a) SEM imaging of SWNT network and (b) schematics of SWNT thin film infrared bolometer. Adapted with permission from ref 8. Copyright 2006 The American Association for the Advancement of Science. (c) Mechanism of electrical response of infrared bolometer, (d) temperature dependence of resistances, and (e) UV−vis−near-IR absorption spectra of networks of unsorted (uns) and 99% SC-SWNTs.

1. INTRODUCTION: SWNT NETWORKS

Single-walled carbon nanotube (SWNT) networks (Figure 1a) provide a unique platform for development of carbon based electronics and photonics because they combine the advantages of the outstanding electrical and optical properties that originate from the one-dimensional (1D) electronic structure of individual SWNTs with the applicability of large area thin film preparation and patterning technologies.[1−3] High performance SWNT thin film based field-effect transistors (FETs), sensors, detectors, solar cells, and light emitting diodes have been already demonstrated, and SWNT thin film applications as transparent conducting coatings for large area displays and smart windows has been significantly advanced.[1,4−21]

Until recently, bulk SWNT materials available for SWNT thin film preparation were composed of a mixture of metallic (MT) and semiconducting (SC) SWNTs of different diameters and chiralities. The presence of MT-SWNTs leads to a degradation of the performance of SWNT thin film based FETs and SWNT thin film infrared bolometers (Figure 1b).[8] In particular, the performance of the bolometer depends on its temperature coefficient of resistance, where TCR = $(1/R)(dR/dT)$ (%);[22] thus a high slope in the $R(T)$ dependence leads to an enhanced TCR and a stronger electrical response of the bolometer to infrared irradiation (Figure 1c). The presence of MT-SWNTs leads to TCR values in the range 0.1−0.3%, too low to be competitive with vanadium oxide (VO_x) based microbolometers, which exhibit TCR in the range 2−4%.[22] On the other hand, some applications, such as transparent conducting coatings may benefit from the presence of MT-SWNTs.

Recently, the solution-based separation of metallic and semiconducting SWNTs has been achieved at a scale that allows the commercial availability of SC-SWNTs,[23] and it was anticipated that thin films made exclusively of SC-SWNTs would behave as intrinsic semiconductors thereby eliminating the deficiencies of the resulting devices, which were previously attributed to the presence of MT-SWNTs. Indeed the bandgap of typical semiconducting SWNTs of diameter, d = 1.5 nm is in the range E_g = 0.6−0.7 eV, which matches the bandgap of conventional semiconductors such as Ge for which E_g = 0.66 eV.[24]

Figure 1d,e compares the temperature dependences of electrical resistance and absorption spectra of 35 nm thick films of unsorted SWNTs, containing a mixture of SC- and MT-SWNTs in the ratio 2:1, and 99% SC-SWNTs containing less than 1% MT-SWNTs. A high degree of separation is confirmed by the disappearance of the M_{11} interband transition originating from the MT-SWNTs (Figure 1e). Thin films of unsorted SWNTs show weak nonmetallic temperature dependence with a slope at 300 K corresponding to a very small activation energy $E_a \approx 10$ meV (Figure 1d).

Films of separated SC-SWNTs annealed in vacuum were expected to have an activation energy corresponding to half the energy gap, $E \approx 0.3$ eV; surprisingly such films show a very small slope with an activation energy of only 24 meV, ∼14 times less than the expected value (Figure 1d). If the S_{11} peak is taken to be excitonic in nature, an even higher activation energy, corresponding to the energy separation between continuum states, is anticipated.[25]

Thus, networks of purely SC-SWNTs do not behave as intrinsic semiconductors with a bandgap corresponding to that of the constituent SC-SWNTs. This Account presents a study of the mechanism of the temperature dependent conductivity in networks of SC-SWNTs previously utilized in a percolation study.[26] There are a number of possible explanations for the nonideal electrical transport in these networks, but the most likely candidate is the presence of midgap states, which originate from defects in the SC-SWNTs.

2. TEMPERATURE DEPENDENCE OF CONDUCTIVITY AS A FUNCTION OF SWNT FILM THICKNESS APPROACHING THE PERCOLATING THRESHOLD

The temperature dependence of the conductivity of SWNT films and its modification as a function of thickness can shed light on the nature of the electrical transport in SWNT networks.[27−32] Films with effective thicknesses in the range 0.5−8 nm were prepared by vacuum filtration of semiconducting SWNT dispersions (IsoNanotubes-S, 99%, Nanointegris),[26] where the

DOI: 10.1021/acs.accounts.5b00107
Acc. Chem. Res. 2015, 48, 2270−2279

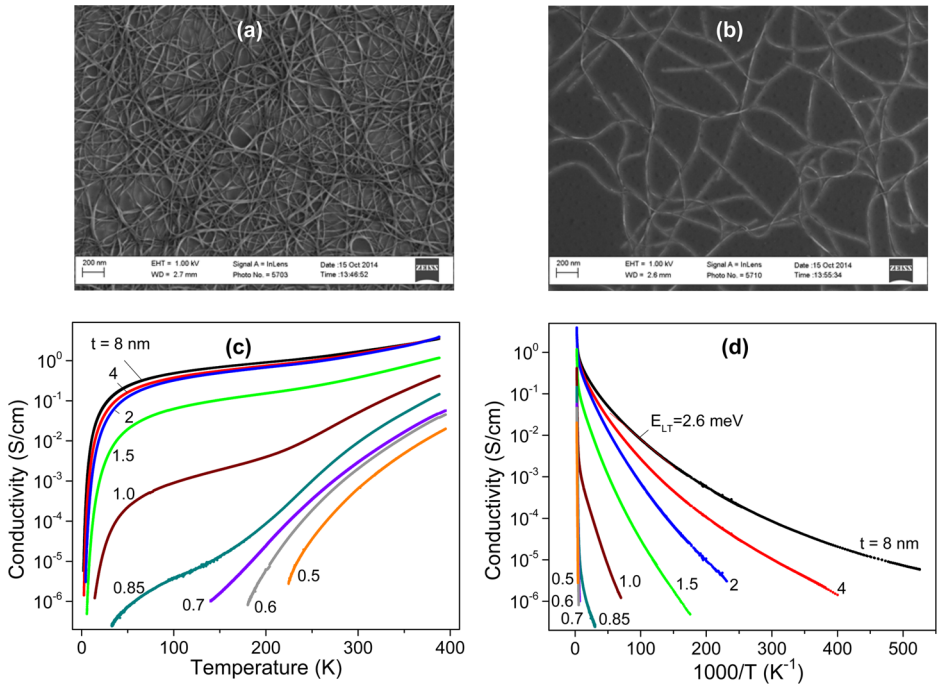

Figure 2. SEM imaging of the film of semiconducting SWNTs of effective thicknesses: (a) 8 nm and (b) 0.5 nm. Dependence of electrical conductivity of the networks of SC-SWNTs of different thicknesses on (c) temperature and (d) inverse temperature.

effective thickness is calculated assuming a SWNT bulk film density of 1.2 g/cm^3.[14,26] Scanning electron microscopy (SEM) images of the SC-SWNT films of different effective thicknesses are presented in Figure 2a,b showing entangled SWNT bundles of diameters 3−10 nm (Supporting Information).[26]

The electrical measurements were conducted on macroscopic channels of the annealed in vacuum SWNT networks of length ∼1 mm and width ∼2 mm supported on alumina membranes, or sapphire or Si substrates with Cr/Au or silver paste electrodes in helium gas atmosphere. The contact resistances were negligible compared with the channel bulk resistances as confirmed by the scaling of the resistance with the length of the channel.

Figure 2 also presents a plot of the electrical conductivity, σ, as a function of temperature (Figure 2c) and inverse temperature (Figure 2d); the latter presentations exemplify the low temperature range, $T < 100$ K. For SWNT film with thicknesses well above percolation threshold (8−2 nm), the conductivity decreases slowly between 400 and 50 K, while between 50 and 2 K, the drop of conductivity exceeds 5 orders of magnitude (Figure 2c). The inverse temperature plot (Figure 2d) shows that the low temperature region is associated with very low energy processes of a variable activation energy, E_{LT} = 2−10 meV, similar in magnitude to the weak temperature dependences reported in literature for networks of mixed MT- and SC-SWNTs.[27−30,32]

We tested several models that were reported to describe the electrical transport in SWNT networks.[27−32] Figure 3 presents a fitting of the experimental data using fluctuation induced tunneling (FIT) model,[33,34] 2D variable range hopping model (2D-VRH),[35] and Efros and Shklovskii VRH model, denoted as ES-VRH, which takes into account Coulomb interactions.[31,36,37] The FIT model was first developed for conducting polymers[33,34] and later applied to the SWNT networks.[27,28,30] This model describes charge transport in a system in which metallic regions are separated by small area (small capacitance) tunneling junctions and the thermal fluctuations modulate the electric field across the junctions affecting the height of the tunneling barrier. The electrical conductance in the FIT model is described by the following expression:

$$\sigma = A \exp\left(\frac{-T_b}{T + T_s}\right) \quad (1)$$

where the prefactor A is assumed to be independent of temperature, T_b is related to the height and shape of the tunneling barrier, and T_s is a characteristic temperature above which thermal fluctuations of the voltage across the tunneling junction became sufficient to modify the tunneling barrier.[33,34] After fitting the experimental temperature dependencies to expression (1), the data were plotted in the form $\log(\sigma)$ vs $1/(T + T_s)$. A good linearization was obtained in the temperature range below ∼70 K where the conductivity changes by 3−4 orders of magnitude for film thicknesses in the range 8−1 nm as can be seen in the left column in Figure 3. The fitting parameters T_b and T_s for different thicknesses are in the range of 50−150 and 2.6−3.7 K, respectively, both increasing with decreasing film thickness. For the film thicknesses below 1 nm, the low temperature range was outside the capabilities of the experiment ($R > 10^{13}$ Ω).

In the case of variable range hopping (VRH) model,[35] the temperature dependence of the conductivity is given by expression 2:

$$\sigma = \sigma_0 \exp\left[-\left(\frac{T_0}{T}\right)^{1/(1+d)}\right] \quad (2)$$

where σ_0 and T_0 are constants with T_0 defined by the density of localized states in the vicinity of the Fermi level and the localization length and d corresponds to the dimensionality of the system. The Efros and Shklovskii ES-VRH model formally requires $d = 1$ to accommodate the Coulomb gap.[36,37] Satisfactory fittings of the SWNT films conductivity to different variations of VRH models were reported recently.[31,32,38]

DOI: 10.1021/acs.accounts.5b00107
Acc. Chem. Res. 2015, 48, 2270−2279

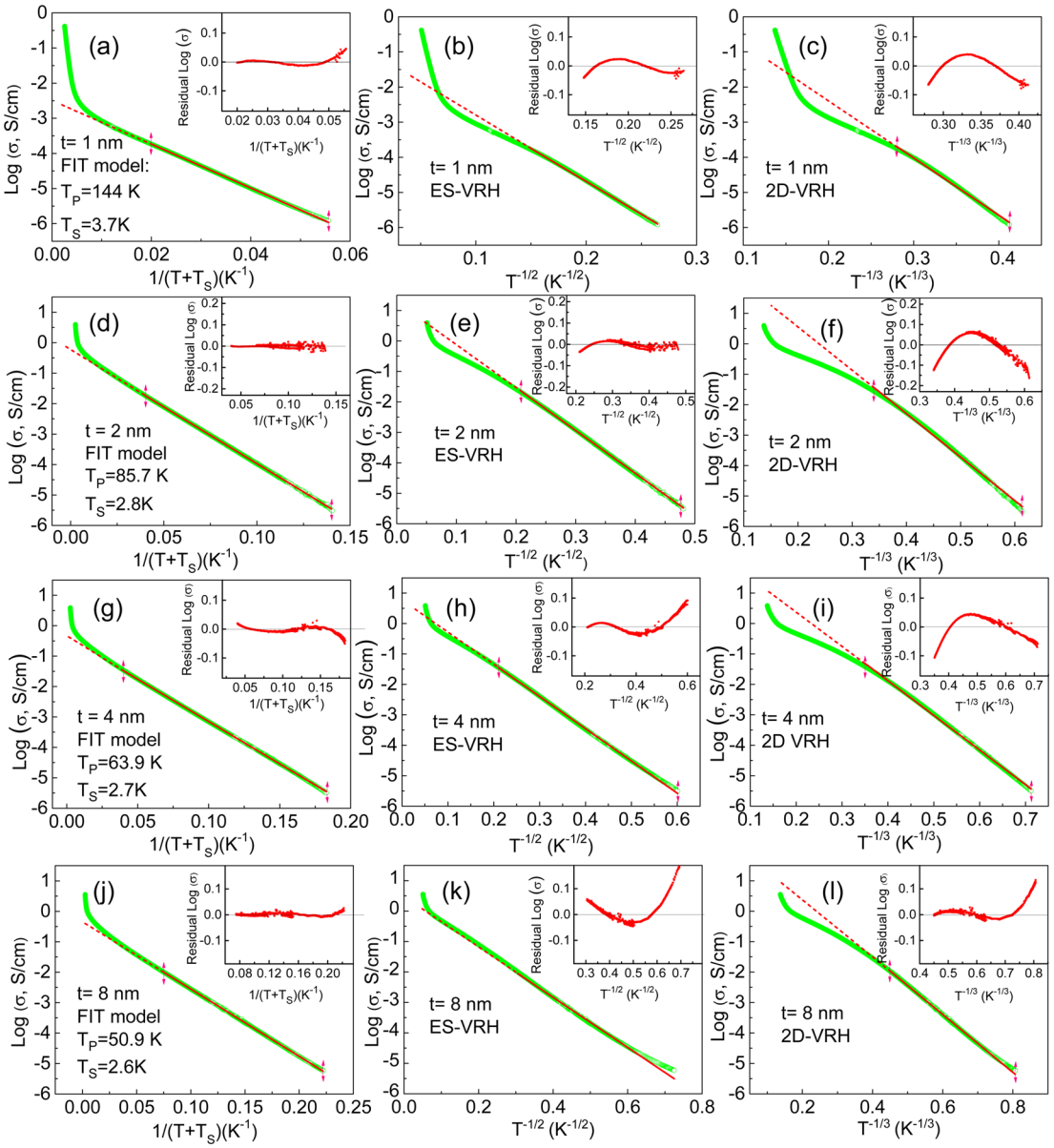

Figure 3. Temperature dependences of conductivity of the films of SC-SWNTs of thicknesses t = 1, 2, 4, and 8 nm (from top to bottom) fitted to FIT model (left column), ES-VRH model (central column), and 2D-VRH model (right column). Insets show the fitting residuals.

Columns 2 and 3 in Figure 3 represent results of VRH fitting for ES-VRH and 2D-VRH cases, respectively; to facilitate direct comparison, the fitting was conducted in the same temperature range as the FIT fitting. First, it should be noted that neither fitting can adequately describe the temperature dependence over the whole temperature range 400−2 K; a strong discrepancy between the fit and the experimental data is observed at temperatures above 50−70 K. In the low temperature range below 50 K, the best fit corresponds to the FIT model (Figure 3, first column), which shows a slight advantage over the ES-VRH model (2nd column), which was reported to provide the best fit in the case of thicker films of SC-SWNTs.[31] More pronounced deviations between the experimental data and the fitting curves were observed for the 2D-VRH (Figure 3, third column) and 3D-VRH models (not shown). Although the temperature range of the fitting is limited, it includes more than 3 orders of magnitude change in the conductivity due to the utilization of highly separated SC-SWNTs.

Despite the different physics behind the theories, both the FIT and VRH models assume tunneling of charge carriers between electronic states residing in the vicinity of Fermi level.[27,28,30−32,38] It should be noted that the SWNT network is a complex system composed of SWNTs connected through intertube junctions, which introduce some degree of disorder and dominate the network resistance.[1,39,40] Nevertheless, the charge carriers contributing to the transport are provided by individual SWNTs, and the conductivity of the network should be proportional to the concentration of these carriers available for transport with a correction to weakly temperature dependent mobility.

In our studies, the SWNT network is formed using SC-SWNTs with average diameter 1.5 eV and bandgap ~0.6−0.7 eV,[14,26] which is similar to the bandgap of germanium.[24] In an ultrapure intrinsic semiconductor of similar bandgap, a decrease in temperature from 400 to 100 K would lead to a decrease of the intrinsic carrier concentration by more than 10 orders of magnitude (limited, in practice, by the concentration of extrinsic carriers),[24] while the

DOI: 10.1021/acs.accounts.5b00107
Acc. Chem. Res. 2015, 48, 2270−2279

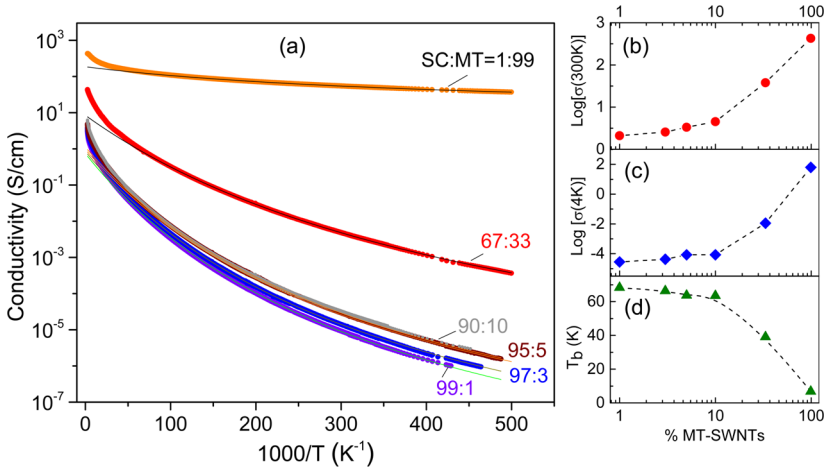

Figure 4. (a) Temperature dependences of conductivity of the films of different ratio of SC- to MT-SWNTs. Lines represent fitting to the FIT model eq 1). Dependence of conductivity at 300 K (b), 4 K (c), and parameter T_b of the FIT model (eq 1) (d) on concentration of MT-SWNTs.

corresponding change of conductivity in an 8 nm thick SC-SWNT film is less than 1 order of magnitude. The availability of Fermi level electronic states can be justified when the SWNT network is formed from a mixture of MT- and SC-SWNTs, only MT-SWNTs, or heavily doped SC-SWNTs, which are capable of providing a finite density of states in the vicinity of the Fermi level.[27−30,32]

In the next two sections, the contributions of residual concentration of MT-SWNTs to the conductance of a predominantly SC-SWNT network and the effect of the doping of SC-SWNTs will be analyzed in order to delineate the nature of the Fermi level electronic states contributing to the weak temperature dependence of conductivity of SC-SWNT networks.

3. CONTRIBUTION OF THE RESIDUAL CONCENTRATION OF MT-SWNTs TO THE CONDUCTANCE OF NETWORKS OF SC-SWNTs

Many of the previous studies made use of SWNTs synthesized by bulk synthetic techniques such as electric arc discharge, laser ablation, or CVD, which produce materials with a statistical 1:2 ratio of MT- to SC-SWNTs. Networks that include a high concentration of MT-SWNTs can form continuous conducting pathways composed solely of MT-SWNTs when the density of the network (film thickness) exceeds the percolation limit,[26,40] and the MT-SWNTs could provide a source of Fermi level electronic states or metallic islands, which can contribute to the FIT or VRH conductance discussed above. The question therefore arises if the samples of 99% pure SC-SWNTs, which are commercially available, are of sufficient semiconducting purity to exclude the contribution of MT-SWNTs to the electrical transport. However, the dopants in classical semiconductors usually occur on the atomic scale, whereas the MT-SWNTs are very large molecules with molecular weights of ∼1 000 000 Da for a 500 nm SWNT,[41] and thus it is difficult to compare the doping in the two classes of materials. For example, the concentration of impurities in classical semiconductors is usually measured as a density, but the concentration of silicon atoms in a pure sample is $\sim 5 \times 10^{22}$ cm^{-3}, whereas the concentration of SWNTs of length 500 nm in a sample is $\sim 6 \times 10^{17}$ cm^{-3}. Given the disparity in the density and aspect ratio of the impurities, it is therefore likely that the effect of atomic dopants or MT-SWNTs on the properties of these materials is quite different. Furthermore, most experiments, including those described in this Account, are performed on SC-SWNTs that contain up to 1% by weight residual metal catalyst.

Samples of 100% separated SC-SWNTs are not yet available, so to shed light on the questions raised above, we utilized dispersions of 99% SC-SWNTs and 99% MT-SWNTs to prepare films of different proportions of SC- to MT-SWNTs at the same effective thickness, t = 8 nm, and the temperature dependent conductivities for this set of films are presented in Figure 4a. It can be seen that there is very little changes in the $\sigma(T)$ dependence as the degree of SC-SWNT separation increases from 90% to 99% where the concentration of MT-SWNTs decreases from 10% to 1%; thus a further improvement in the separation might not change the shape of the $\sigma(T)$ curve and this conclusion was supported when we tested a film made of commercially available 99.7% SC-SWNTs.

Figure 4b,c supports the validity of such an extrapolation suggesting that the values of σ(300K) and σ(4K) approach saturation at concentrations of MT-SWNTs below 10%. The resulting plot of $\sigma(T)$ can be fitted satisfactorily to the FIT model; the fitting parameter T_b also shows a saturation below a concentration of 10% MT-SWNTs supporting the observed trend (Figure 4d). This suggest that the presence of residual amounts of MT-SWNTs at concentrations below 10% does not cause the observed weak temperature dependence of conductivity and suggests that the MT-SWNTs are not the source of the Fermi level electronic states responsible for FIT or VRH transport at low temperatures.

4. CONTRIBUTION OF DOPING

It is well-known that SWNTs are susceptible to environmental p-doping due to exposure to oxygen and water vapors in the ambient atmosphere, and as a result of defects introduced by the purification procedure and other types of solution based processing.[42] The p-doping can shift the Fermi level of SC-SWNTs toward the edge of the valence band thus providing the source of low energy excitation leading to the weak temperature dependence of the electrical conductivity. In order to eliminate or minimize the effect of the doping the SWNT films were annealed in a vacuum of 10^{-7} Torr at 350 °C for 6 h, quickly transferred to the temperature probe for conductivity measurements and in situ annealed at 110 °C for 12 h to compensate for the effect of the short atmospheric exposure. To evaluate whether the annealing procedure is sufficient for restoring the intrinsic state of semiconducting SWNTs, the SWNT films of different thicknesses were transferred onto p-doped Si substrate with 300 nm gate

DOI: 10.1021/acs.accounts.5b00107
Acc. Chem. Res. 2015, 48, 2270−2279

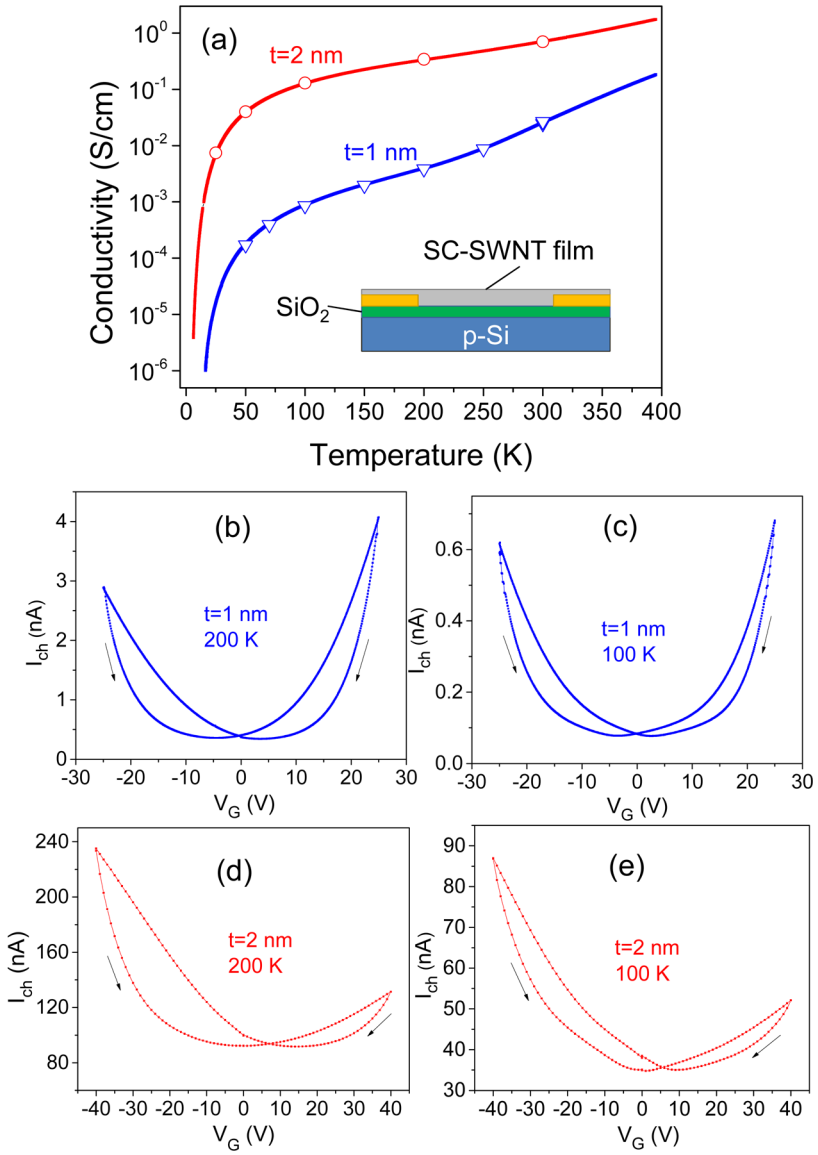

Figure 5. Investigation of degree of doping of SC-SWNTs using FET configuration: (a) temperature dependent conductivity of SC-SWNT networks; open symbols correspond to the conductivity of FETs in neutrality points; (inset) schematic of SC-SWNT thin film FET; (b−e) gate voltage dependences of FET channel current for the thicknesses of SWNT thin film of 1 nm (b,c) and 2 nm (d,e) at temperatures 200 K (b,d) and 150 K (c,e).

dielectric SiO_2 layer and prepatterned Cr/Au source and drain electrodes in a FET configuration as presented schematically in Figure 5a (inset). The corresponding $\sigma(T)$ dependences for 2 and 1 nm thick 99% SC-SWNT films are presented in Figure 5a as lines and are in agreement with the data observed for the SC-SWNT films supported on alumina (Figure 2) or sapphire substrates.

In addition, gate voltage (V_G) dependences of the channel current, I_{ch}, at bias voltage V_{ch} = 1 V were measured at different temperatures, and the results of the gate voltage scans are presented in Figure 5b−e. The scans show the hysteretic behavior typical of SWNT thin film FETs, which has been ascribed to the presence of localized charges trapped at the SWNT/SiO_2 interface,[4] but the shape of $I_{ch}(V_G)$ loops is symmetrical around V_G = 0. The conductivity of the FET channel at the neutrality point at minimum current corresponds to the intrinsic state of the SC-SWNT film; the data corresponding to these intrinsic conductivities were added to the plot in Figure 5a as open symbols and match the $\sigma(T)$ dependences obtained at zero gate voltage (Figure 5a). Thus, it can be concluded that the weak temperature dependence of the electrical conductivity of SC-SWNTs is not associated with SWNT doping and corresponds to intrinsic behavior of the SC-SWNT network.

5. MECHANISM OF CONDUCTIVITY OF THE NETWORKS OF SEMICONDUCTING SWNTs AND CONTRIBUTION OF MIDGAP STATES

In conventional semiconductors, low temperature electrical transport is ascribed to the hopping of the carriers between the midgap states originating from lattice defects or residual impurities and located within energy κT of the Fermi level.[35] In the SWNT networks of mixed SC- and MT-SWNTs, the electrical transport was typically analyzed using the FIT or VRH models and the excess conductivity ascribed to Fermi level electronic states provided by the MT-SWNTs.[27,28,30−32,38] As shown in sections 3 and 4, the observed low temperature electrical behavior of the network of SC-SWNTs is unlikely to be explained by the contribution of the residual concentration of MT-SWNTs or the effect of doping of SC-SWNTs. Thus, the

DOI: 10.1021/acs.accounts.5b00107
Acc. Chem. Res. 2015, 48, 2270−2279

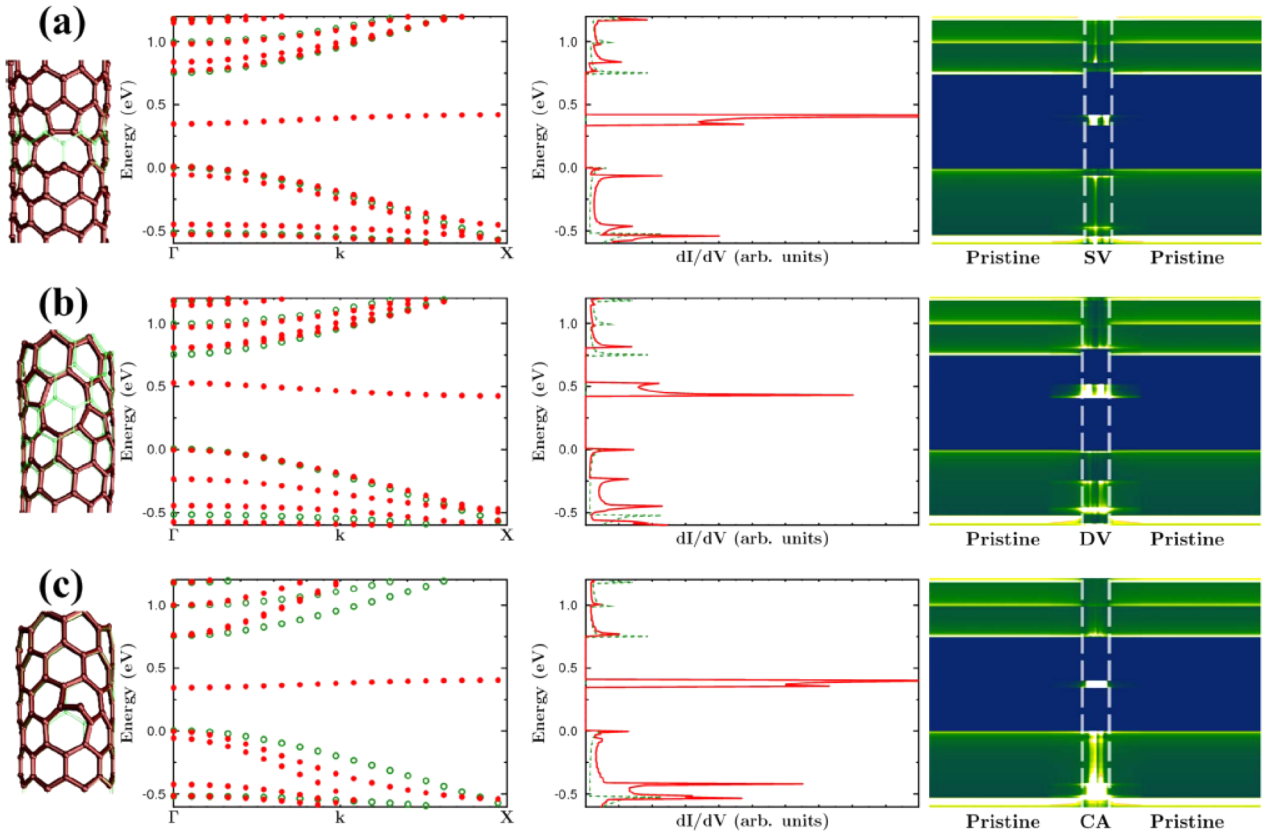

Figure 6. From the left to the right, reconstructed atomic structures of a (a) single vacancy, (b) double vacancy, and (c) a single carbon adatom in the lowest-energy configuration, the corresponding band structures, local densities of states, and the simulated dI/dV scans. Green bonds and curves correspond to the pristine nanotubes; red to the defected ones. Zero energy corresponds to the valence-band edge of the pristine system. Adapted with permission from ref 52. Copyright 2009 The American Physical Society.

required midgap states should originate from the SC-SWNTs themselves.

There are a number of specific defects in the SWNT walls discussed in the literature that disrupt the electronic band structure of ideal SWNTs, and some of those defects give rise to the midgap states.[43−52] According to calculation, single vacancy, double vacancy, and carbon adatom defects each provide a single peak in the middle of the bandgap with a band dispersion at the level 50−70 meV (Figure 6).[52]

Other types of defects such as triple vacancies and Stone−Wales are capable of modifying locally the width of a bandgap.[52] Some of the modeling was done to account for experimentally observed features in low-temperature scanning tunneling microscopy and spectroscopy studies conducted on Ar-ion irradiated SWNTs,[52] although even in pristine SWNTs a significant presence of defects and disorder was revealed experimentally by the Coulomb blockade observed in low temperature electrical measurements,[53−55] selective electrochemical deposition imaging,[47] tip-enhanced Raman spectroscopy,[56] and high resolution photocurrent spectroscopy.[25]

The origin of the defects observed in pristine SWNTs has not been established; the defects may be formed during the SWNT synthesis or solution-based processing, which often includes air oxidation, acid treatment, solution based tip sonication, and centrifugation during exfoliation and sorting.[57] Interaction with the substrate, bending, and deformation of the entangled SWNTs forming the network can also affect the electronic density of states.[49,53,54,58] It is widely accepted that in high quality intrinsic SWNTs the defects are spaced by a distance of 1 μm or larger, which exceeds the typical hopping length for conventional semiconductors. Recently, experimental indications of a higher density of defects with separations of 300−30 nm were observed in SWNTs of different origins.[25,47,55,56] For example, tip-enhanced Raman spectroscopic imaging of localized defects led to an empirical relationship between the defect separation length (L_D) and the ratio of the intensities of Raman G-band I_G and D-band I_D: $L_D = [0.5\ \text{nm}](I_G/I_D)$.[56] With typical ratio $I_G/I_D = 50−70$ in the highly separated SC-SWNTs employed in this study, $L_D = 25−35$ nm well within the typical VRH distance. The hopping of carriers may also occur between defect sites of neighboring SWNTs within the bundles forming the SWNT network; intrabundle hopping would significantly decrease the hopping distance for typical bundle diameters of 3−10 nm.

Figure 7a presents the temperature dependences of conductivity of SC-SWNT films of several thicknesses fitted to the FIT model at low temperatures. The qualitative picture of low temperature (LT) transport in the network of SC-SWNTs is presented in Figure 7c.

At low temperatures the concentration of thermally activated electrons and holes in the conduction and valence bands is infinitesimal and the only conductance channel corresponds to the hopping of the charge carriers along the midgap states followed by tunneling across the junction. The intertube tunneling is still a bottleneck for the overall transport through the network[1,39,40] as indicated by the agreement between $\sigma(T)$ dependence and the FIT model.[27−30,33,34]

The extension of the fitting curves to the high temperature range in Figure 7a shows a deviation from the experimental $\sigma(T)$

DOI: 10.1021/acs.accounts.5b00107
Acc. Chem. Res. 2015, 48, 2270−2279

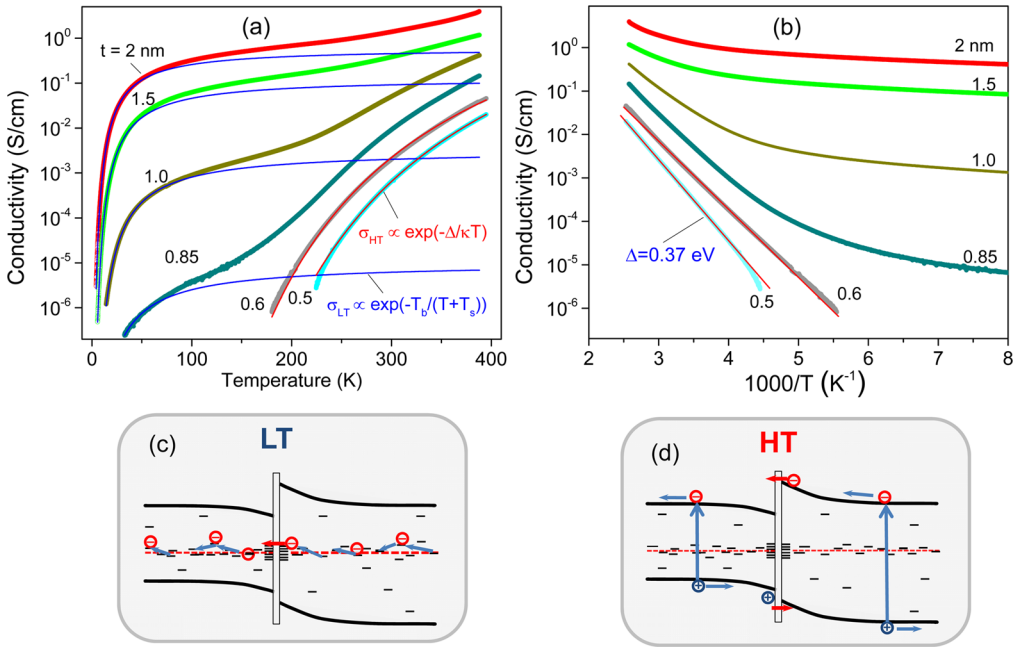

Figure 7. Dependence of conductivity on (a) temperature and (b) inverse temperature and fitting of the low temperature range to fluctuation induced tunneling model eq 1 and high temperature range to activation across the bandgap of SC-SWNTs. (c) Illustration of low temperature (LT) electrical transport involving midgap states of SC-SWNTs and (d) high temperature transport involving thermal activation across the bandgap.

dependencies thus revealing an additional contribution that becomes more pronounced with decreasing film thickness. The high temperature activation contribution was reported recently for the case of the films of unsorted SWNTs and was ascribed to the thermionic emission across Schottky barriers formed at the junctions of MT- and SC-SWNTs.[32]

Figure 7c expands the high temperature part of the Arrhenius plot presented in Figure 2d revealing the appearance of a thermally activated process with activation energy E_{HT} as high as 0.37 eV that becomes apparent when the film thickness approaches the percolation threshold (t = 0.6 and 0.5 nm). This additional high temperature (HT) contribution can be associated with increasing population of intrinsic carriers thermally activated across the bandgap, which are available for band transport along the individual nanotube followed by the tunneling or thermionic emission across the barrier at the intertube junction (Figure 7d). The transition from LT to HT behavior cannot be accurately described by a single activation process for all thicknesses and temperatures; the variable activation energy may arise from the distribution of the energies of the defect states within the bandgap.

6. CONCLUSIONS

While the recently achieved commercial separation of SC- and MT-SWNTs has facilitated progress toward the development of SWNT nanoelectronic and nanophotonics applications, networks of separated SC-SWNTs do not approach the behavior of intrinsic semiconductors of similar bandgap such as germanium. The observed weak temperature dependence of the electrical conductivity of SC-SWNT networks may require the presence of processing-induced midgap states, which provide low-energy excitations contributing to hopping conductance along the nanotubes following fluctuation induced tunneling or hopping across the intertube junctions. The appearance of midgap states is not unusual even in highly pure conventional semiconductors, but what is unusual is the extent of their contribution to the electrical transport in networks of SC-SWNTs over a wide temperature range.

The progress of the semiconductor industry has been driven by the continuous improvement of materials purity, which in the case of Si has been raised from 99.99% in the 1950s to its current level of more than 99.9999999%. The controlled introduction of impurities with energy states that lie within the bandgap of Si and Ge has allowed the exponential growth of the semiconductor industry as a result of its success in developing high density integrated circuits and extremely sensitive infrared photodetectors.[22,24] The current state of SWNT purity in the best separated materials is difficult to estimate but is probably 99.99% to 99.999% (4N−5N) corresponding to one defect per 50 to 500 nm of the SWNT length, and this obviously affects the applications of these materials. While this issue does not necessarily limit directly synthesized SC-SWNTs, the question remains as to whether a SWNT process can produce SC-SWNTs that are free of midgap states, since the present results suggest that this will allow the realization of semiconducting SWNT networks that mimic the properties of individual SC-SWNTs and traditional semiconductors.

■ ASSOCIATED CONTENT

Supporting Information

The Supporting Information is available free of charge on the ACS Publications website at DOI: 10.1021/acs.accounts.5b00107.

AFM images and temperature dependences of conductivity of SWNT networks of different bundle sizes (PDF)

■ AUTHOR INFORMATION

Corresponding Authors

*E-mail: mitkis@engr.ucr.edu.
*E-mail: haddon@ucr.edu.

Notes

The authors declare no competing financial interest.

DOI: 10.1021/acs.accounts.5b00107
Acc. Chem. Res. 2015, 48, 2270−2279

Biographies

Mikhail Itkis earned a B.S. degree in Physics from the Moscow Institute of Physics and Technology and a Ph.D. in Physics from the Institute of Radio Engineering & Electronics, Russian Academy of Sciences. His research interests cover physics, material science, and applications of low dimensional materials. He is currently a Research Professor at the University of California, Riverside. In 2011, he was recognized by Thomson Reuters as a world top 100 chemist of the past decade.

Aron Pekker obtained his M.S. in 2005 and Ph.D. in 2011 in Physics from the Budapest University of Technology and Economics (Hungary) with Prof. Katalin Kamaras. He was a postdoctoral scholar in the group of Prof. Robert C. Haddon at the University of California Riverside from 2011 to 2014. Currently he is a postdoctoral scholar at the Wigner Research Centre for Physics (Hungary).

Xiaojuan Tian recently obtained her Ph.D. degree in Chemical Engineering at the University of California, Riverside, in the Haddon research group. She received her B.S. from Nankai University in China. Her current research focus is chemical processing and applications of graphite nanoplatelets and carbon nanotubes.

Elena Bekyarova obtained her Ph.D. degree in Chemistry from the Bulgarian Academy of Sciences. She is currently an Associate Researcher at the University of California, Riverside. Her research interests include synthesis, properties, and applications of carbon nanotubes and graphene with particular focus on the chemistry of these materials and modification of their electronic and magnetic properties.

Robert Haddon is Distinguished Professor in the Departments of Chemistry and Chemical & Environmental Engineering and Director of the Center for Nanoscale Science and Engineering at University of California, Riverside.

■ ACKNOWLEDGMENTS

We gratefully acknowledge the financial support of the National Science Foundation under contract ECCS-1404671.

■ REFERENCES

(1) Gruner, G. Carbon Nanotube Films for Transparent and Plastic Electronics. *J. Mater. Chem.* **2006**, *16*, 3533−3539.
(2) Jorio, A.; Dresselhaus, M. S.; Dresselhaus, G. *Carbon Nanotube. Advanced Topics in the Synthesis, Structure, Properties and Applications*; Springer-Verlag: Berlin, Germany, 2008; Vol. *111*.
(3) Avouris, P.; Freitag, M.; Perebeinos, V. Carbon Nanotube Photonics and Optoelectronics. *Nat. Photonics* **2008**, *2*, 341−350.
(4) Bradley, K.; Gabriel, J.-C. P.; Briman, M.; Star, A.; Gruner, G. Charge Transfer from Ammonia Physisorbed on Nanotubes. *Phys. Rev. Lett.* **2003**, *91*, 218301.
(5) Wu, Z.; Chen, Z.; Du, X.; Logan, J. M.; Sippel, J.; Nikolou, M.; Kamaras, K.; Reynolds, J. R.; Tanner, D. B.; Hebard, A. F.; Rinzler, A. G. Transparent, Conductive Carbon Nanotube Films. *Science* **2004**, *305*, 1273−1276.
(6) Kaempgen, M.; Duesberg, G. S.; Roth, S. Transparent Carbon Nanotube Coating. *Appl. Surf. Sci.* **2005**, *252*, 425−429.
(7) Snow, E. S.; Perkins, F. K.; Houser, E. J.; Badescu, S. C.; Reinecke, T. L. Chemical Detection with a Single-Walled Carbon Nanotube Capacitor. *Science* **2005**, *307*, 1942−1945.
(8) Itkis, M. E.; Borondics, F.; Yu, A.; Haddon, R. C. Bolometric Infrared Photoresponse of Suspended Single-Walled Carbon Nanotube Films. *Science* **2006**, *312*, 413−416.
(9) Rowell, M. W.; Topinka, M. A.; McGehee, M. D.; Prall, H. J.; Dennler, G.; Sariciftci, N. S.; Hu, L. B.; Gruner, G. Organic Solar Cells with Carbon Nanotube Network Electrodes. *Appl. Phys. Lett.* **2006**, *88*, 233506.
(10) Zhang, D.; Ryu, K.; Liu, X.; Polikarpov, E.; Ly, J.; Tompson, M. E.; Zhou, C. Transparent, Conductive, and Flexible Carbon Nanotube Films and Their Applications in Organic Light-Emitting Diodes. *Nano Lett.* **2006**, *6*, 1880−1886.
(11) Bekyarova, E.; Kalinina, I.; Itkis, M. E.; Beer, L.; Cabrera, N.; Haddon, R. C. Mechanism of Ammonia Detection by Chemically Functionalized Single-Walled Carbon Nanotubes: In Situ Electrical and Optical Study of Gas Analyte Detection. *J. Am. Chem. Soc.* **2007**, *129*, 10700−10706.
(12) Itkis, M. E.; Yu, A.; Haddon, R. C. Single-Walled Carbon Nanotube Thin Film Emitter-Detector Integrated Optoelectronic Device. *Nano Lett.* **2008**, *8*, 2224−2228.
(13) Kauffman, D. R.; Star, A. Carbon Nanotube Gas and Vapor Sensors. *Angew. Chem., Int. Ed.* **2008**, *47*, 6550−6570.
(14) Wang, F.; Itkis, M. E.; Haddon, R. C. Enhanced Electromodulation of Infrared Transmittance in Semitransparent Films of Large Diameter Semiconducting Single-Walled Carbon Nanotubes. *Nano Lett.* **2010**, *10*, 937−942.
(15) Wadhwa, P.; Liu, B.; McCarthy, M. A.; Wu, Z.; Rinzler, A. G. Electronic Junction Control in a Nanotube-Semiconductor Schottky Junction Solar Cell. *Nano Lett.* **2010**, *10*, 5001−5005.
(16) Hu, L. B.; Hecht, D. S.; Gruner, G. Carbon Nanotube Thin Films: Fabrication, Properties, and Applications. *Chem. Rev.* **2010**, *110*, 5790−5844.
(17) Baetens, R.; Jelle, B. P.; Gustavsen, A. Properties, Requirements and Possibilities of Smart Windows for Dynamic Daylight and Solar Energy Control in Buildings: A State-of-the-Art Review. *Sol. Energy Mater. Sol. Cells* **2010**, *94*, 87−105.
(18) Zhang, J.; Fu, Y.; Wang, C.; Chen, P.; Liu, Z.; Wei, W.; Wu, C.; Thompson, M. E.; Zhou, C. Separated Carbon Nanotubes Macroelectronics for Active Matrix Organic Light-Emitting Diode Displays. *Nano Lett.* **2011**, *11*, 4852−4858.
(19) McCarthy, M. A.; Liu, B.; Donoghue, E. P.; Kravchenko, I.; Kim, D. Y.; So, F.; Rinzler, A. G. Low-Voltage, Low-Power, Organic Light-Emitting Transistors for Active Matrix Displays. *Science* **2011**, *332*, 570−573.
(20) Gwinner, M. C.; Jakubka, F.; Gannott, F.; Sirringhaus, H.; Zaumseil, J. Enhanced Ambipolar Charge Injection with Semiconducting Polymer/Carbon Nanotube Thin Films for Light-Emitting Transistors. *ACS Nano* **2012**, *6*, 539−548.
(21) Wang, F.; Itkis, M. E.; Bekyarova, E.; Haddon, R. C. Charge Compensated, Semiconducting Single-Walled Carbon Nanotube Thin Film as an Electrically Configurable Optical Medium. *Nat. Photonics* **2013**, *7*, 459−465.
(22) Rogalski, A. *Infrared Detectors*, 2 ed.; CRS Press: Boca Raton, FL, 2011.
(23) Arnold, M. S.; Green, A. A.; Hulvat, J. F.; Stupp, S. I.; Hersam, M. C. Sorting Carbon Nanotubes by Electronic Structure Using Density Differentiation. *Nat. Nanotechnol.* **2006**, *1*, 60−65.
(24) Sze, S. M. *Physics of Semiconductor Devices*, 2 ed.; Wiley-Interscience: New York, 1981.
(25) Comfort, E. S.; Jones, D. A.; Malapanis, A.; Robinson, Z. R.; Fishman, M. T.; Lee, J. U. Spectroscopy of Strongly Localized Excitons and Band-Gap States in Semiconducting Single-Walled Carbon Nanotubes. *Phys. Rev. B: Condens. Matter Mater. Phys.* **2011**, *83*, 081401.
(26) Tian, X.; Moser, M. L.; Pekker, A.; Sarkar, S.; Ramirez, J.; Bekyarova, E.; Itkis, M. E.; Haddon, R. C. Effect of Atomic Interconnects on Percolation in Single-Walled Carbon Nanotube Thin Film Networks. *Nano Lett.* **2014**, *14*, 3930−3937.
(27) Kaiser, A. B.; Dusberg, G.; Roth, S. Heterogeneous Model for Conduction in Carbon Nanotubes. *Phys. Rev. B: Condens. Matter Mater. Phys.* **1998**, *57*, 1418−1421.
(28) Kaiser, A. B. Electronic Transport Properties of Conduction Polymers and Carbon Nanotubes. *Rep. Prog. Phys.* **2001**, *64*, 1−49.
(29) Skakalova, V.; Kaiser, A. B.; Woo, Y. S.; Roth, S. Electronic Transport in Carbon Nanotubes: From Individual Nanotubes to Thin and Thick Networks. *Phys. Rev. B: Condens. Matter Mater. Phys.* **2006**, *74*, 085403.
(30) Barnes, T. M.; Blackburn, J. L.; van de Lagemaat, J.; Coutts, T. J.; Heben, M. J. Reversibility, Dopant Desorption, and Tunneling in the

DOI: 10.1021/acs.accounts.5b00107
Acc. Chem. Res. 2015, 48, 2270−2279

Temperature Dependent Conductivity of Type Separated, Conductive Carbon Nanotube Networks. *ACS Nano* **2008**, *2*, 1968−1976.
(31) Yanagi, K.; Udoguchi, H.; Sagitani, S.; Oshima, Y.; Takenobu, T.; Kataura, H.; Ishida, T.; Matsuda, K.; Maniwa, Y. Transport Mechanisms in Metallic and Semiconducting Single-Wall Carbon Nanotube Networks. *ACS Nano* **2010**, *4*, 4027−4032.
(32) Ravi, S.; Kaiser, A. B.; Bumby, C. W. Charge Transport in Surfactant - Free Single Walled Carbon Nanotube Networks. *Phys. Status Solidi B* **2013**, *250*, 1463−1467.
(33) Sheng, P. Fluctuation - Induced Tuneling Conduction in Disordered Materials. *Phys. Rev. B: Condens. Matter Mater. Phys.* **1980**, *21*, 2180−2195.
(34) Sheng, P.; Sichel, E. K.; Gittleman, J. I. Fluctuation - Induced Tunneling Conduction in Carbon - Polyvinylchloride Composites. *Phys. Rev. Lett.* **1978**, *40*, 1197−1200.
(35) Mott, N. *Conduction in Non-Crystalline Materials*; Clarendon Press: Oxford, UK, 1987.
(36) Shklovskii, B. I.; Efros, A. *Electronic Properties of Doped Semiconductors*; Springe-Verlag: Berlin, Germany,1984.
(37) Fogler, M. M.; Teber, S.; Shklovskii, B. I. Variable-Range Hopping in Quasi-One-Dimensional Electron Crystals. *Phys. Rev. B: Condens. Matter Mater. Phys.* **2004**, *69*, 035413.
(38) Han, Z. J.; Ostrikov, K. Controlled Electronic Transport in Single-Walled Carbon Nanotube Networks: Selecting Electron Hopping and Chemical Doping Mechanisms. *Appl. Phys. Lett.* **2010**, *96*, 233115.
(39) Nirmalraj, P. N.; Lyons, P. E.; De, S.; Coleman, J. N.; Boland, J. J. Electrical Connectivity in Single-Walled Carbon Nanotube Networks. *Nano Lett.* **2009**, *9*, 3890−3895.
(40) Topinka, M. A.; Rowell, M. W.; Goldhaber-Gordon, D.; McGehee, M. D.; Hecht, D. S.; Gruner, G. Charge Transport in Interpenetrating Networks of Semiconducting and Metallic Carbon Nanotubes. *Nano Lett.* **2009**, *9*, 1866−1871.
(41) Hamon, M. A.; Hu, H.; Bhowmik, P.; Niyogi, S.; Zhao, B.; Itkis, M. E.; Haddon, R. C. End-Group and Defect Analysis of Soluble Single-Walled Carbon Nanotubes. *Chem. Phys. Lett.* **2001**, *347*, 8−12.
(42) Collins, P. G.; Bradley, K.; Ishigami, M.; Zettl, A. Extreme Oxygen Sensitivity of Electronic Properties of Carbon Nanotubes. *Science* **2000**, *287*, 1801−1804.
(43) Kim, P.; Odom, T. W.; Huang, J.-L.; Lieber, C. M. Electronic Density of States of Atomically Resolved Single-Walled Carbon Nanotubes: Van Hove Singularities and End States. *Phys. Rev. Lett.* **1999**, *82*, 1225−1228.
(44) Orlikowski, D.; Nardelli, M. B.; Bernhole, J.; Roland, C. Theoretical STM Signatures and Transport Properties of Native Defects in Carbon Nanotubes. *Phys. Rev. B: Condens. Matter Mater. Phys.* **2000**, *61*, 14194−14203.
(45) Ouyang, M.; Huang, J.-L.; Cheung, C. L.; Lieber, C. M. Atomically Resolved Single-Walled Carbon Nanotube Intramolecular Junction. *Science* **2001**, *291*, 97−100.
(46) Charlier, J.-C. Defects in Carbon Nanotubes. *Acc. Chem. Res.* **2002**, *35*, 1063−1069.
(47) Fan, Y. W.; Goldsmith, B. R.; Collins, P. G. Identifying and Counting Point Defects in Carbon Nanotubes. *Nat. Mater.* **2005**, *4*, 906−911.
(48) Lee, S.; Kim, G.; Kim, H.; Choi, B.-Y.; Lee, J.; Jeong, B. W.; Ihm, J.; Kuk, Y.; Kahng, S.-J. Paired Gap States in a Semiconducting Carbon Nanotube: Deep and Shallow Levels. *Phys. Rev. Lett.* **2005**, *95*, 166402.
(49) Gao, B.; Glattli, D. C.; Placais, B.; Bachtold, A. Cotunneling and One-Dimensional Localization in Individual Disordered Single-Wall Carbon Nanotubes: Temperature Dependence of the Intrinsic Resistance. *Phys. Rev. B: Condens. Matter Mater. Phys.* **2006**, *74*, 085410.
(50) Krasheninnikov, A. V.; Banhart, F. Engineering of Nanostructured Carbon Materials with Electron or Ion Beams. *Nat. Mater.* **2007**, *6*, 723−733.
(51) Goldsmith, B. R.; Coroneus, J. G.; Khalap, V. R.; Kane, A. A.; Weiss, G. A.; Collins, P. G. Conductance-Controlled Point Functionalization of Single-Walled Carbon Nanotubes. *Science* **2007**, *315*, 77−81.
(52) Tolvanen, A.; Buchs, G.; Ruffieux, P.; Gröning, P.; Gröning, O.; Krasheninnikov, A. V. Modifying the Electronic Structure of Semiconducting Single-Walled Carbon Nanotubes by Ar^+ Ion Irradiation. *Phys. Rev. B: Condens. Matter Mater. Phys.* **2009**, *79*, 125430.
(53) Bezryadin, A.; Verschueren, A. R. M.; Tans, S. J.; Dekker, C. Multiprobe Transport Experiments on Individual Single-Wall Carbon Nanotubes. *Phys. Rev. Lett.* **1998**, *80*, 4036−4039.
(54) McEuen, P. L.; Bockrath, M.; Cobden, D. H.; Yoon, Y.-G.; Louie, S. G. Disorder, Pseudospins, and Backscattering in Carbon Nanotubes. *Phys. Rev. Lett.* **1999**, *83*, 5098−5101.
(55) Stokes, P.; Khondaker, S. I. Evaluating Defects in Solution-Processed Carbon Nanotube Devices via Low-Temperature Transport Spectroscopy. *ACS Nano* **2010**, *4*, 2659−2666.
(56) Georgi, C.; Hartschuh, A. Tip-Enhanced Raman Spectroscopic Imaging of Localized Defects in Carbon Nanotubes. *Appl. Phys. Lett.* **2010**, *97*, 143117.
(57) Niyogi, S.; Hamon, M. A.; Perea, D.; Kang, C. B.; Zhao, B.; Pal, S. K.; Wyant, A. E.; Itkis, M. E.; Haddon, R. C. Ultrasonic Dispersions of Single-Walled Carbon Nanotubes. *J. Phys. Chem. B* **2003**, *107*, 8799−8804.
(58) Fuhrer, M. S.; Nygard, J.; Shih, L.; Forero, M.; Yoon, Y.-G.; Mazzoni, M. S. C.; Choi, H. J.; Ihm, J.; Louie, S. G.; Zettl, A.; McEuen, P. L. Crossed Nanotube Junctions. *Science* **2000**, *288*, 494−497.

DOI: 10.1021/acs.accounts.5b00107
Acc. Chem. Res. 2015, 48, 2270−2279